CHALMERS
UNIVERSITY OF TECHNOLOGY

Residual Capacity of RC Beams Subjected to Impact Loading

In Proceedings of the 90th Shock and Vibration Symposium, Shock and Vibration Exchange, www.savecenter.org, Atlanta, Georgia, November 2019.

Residual Capacity of RC Beams Subjected to Impact Loading

Morgan Johansson[a,b*], Joosef Leppänen[b], Mathias Flansbjer[b,c], Fabio J. Lozano[a], and Josef A. Makdesi[d]

[a]Norconsult AB
Theres Svenssons gata 11, 417 55 GÖTEBORG, Sweden
*Corresponding author: morgan.johansson@norconsult.com

[b]Chalmers University of Technology
SE-412 96 GÖTEBORG, Sweden

[c]RISE Research Institutes of Sweden
Box 857, SE-501 15 BORÅS, Sweden

[d]Sweco
Box 5397, SE-402 28 GÖTEBORG, Sweden

Reinforced concrete (RC) is commonly used for protectives structures and how impact loading affects the structural response is an important issue. Knowledge gained from static loading is often also used in the design of impulse loaded structures. However, the response of an impact loaded structural member may be very different compared to a statically loaded one. Consequently, the plastic deformation capacity and failure modes of concrete structures can be different when subjected to impact loads; and hence it is not sure that the observations obtained from static loading are also valid for impact loading.

The aim of this paper is to study the residual capacity in reinforced concrete beams after they were first subjected to impact loading. Drop weight impact tests of 12 beams were carried out and the residual capacity were tested in three-point bending after the impact; six beams were statically tested as references. The beams were simply supported with a span length of 1.0 m and dimensions 0.1 x 0.1 x 1.18 m. The drop weight had a mass of 10.1 kg and was dropped from heights 2.5 m or 5.0 m. A high-speed camera, with 5 000 fps, was used during the impact tests. From the images obtained, digital image correlation (DIC) analyses were conducted, and deformations and crack propagation of the beams were measured.

The results showed, that the crack formation depended on the type of loading. For the statically loaded reference beams, mainly bending cracks occurred, while for impact loaded beams, distinctive diagonal shear cracks also formed below the impact zone and approximately midway to the support. In addition, initial bending cracks developed in the upper part of the beam during impact; which later closed.

The total plastic deformation capacity increased for beams first subjected to drop weight impact tests from a drop height of 5.0 m. For the lower drop height, the plastic deformation capacity was in the same order of magnitude as for the statically loaded reference beams. Bending failure were expected in all beams. However, one of the impact tested beams exhibited a shear failure at a significantly reduced load level when it was afterwards subjected to static loading; indicating that there might be a risk of reduced residual load capacity for impact loaded structures.

INTRODUCTION

Reinforced concrete is commonly used for protective structures and how impulse loading affects different types of concrete structures is hence an issue of importance. Generally, impulse loading is caused by the blast wave from an explosion or an impact from an object hitting the structure with a given velocity. The properties of such loads may differ considerably, but the structural response of the affected structure is in many ways similar. Hence, when studying the structural response of an impulse loaded structure it is often possible to use a more simplified test set-up of an impact loading than that necessary to simulate the blast load generated by an explosion.

Understanding the response of reinforced concrete structures subjected to impulse loading is essential in the design of protective structures. However, the conceptual structural response of such a structure may differ considerably compared when statically loaded. One reason for this is due to so called strain rate effects, affecting the material properties of the loaded structure; [1], [2]. Another reason is so called wave propagation effects; i.e. the transformation of information within the loaded structure may cause it to respond differently in both a local and a global sense; [3]-[5]. Even so it is common to base the design of impulse loaded structures on knowledge gained from static loading; e.g. the maximum moment or plastic deformation capacity, [6]-[8].

The design of impulse loaded structures often relies upon large plastic deformation capacities; i.e. the energy consumption of the structure is handled by large deformations rather than large internal forces. Hence, it is essential that the plastic deformation capacity used in the design is also relevant for the actual load case. However, since the structural response of an impulse loaded structure may be different compared to when statically loaded, the plastic deformation capacity and failure modes of the structure may also be different when subjected to impulse loading. Hence, it is of interest to make sure that the observations obtained from static loading, regarding plastic deformation capacity, are also valid for dynamic loading.

The aim of this paper is to investigate how the plastic deformation capacity of reinforced concrete beams is affected by impulse loading. To simplify, drop weight impact tests were used to simulate the impulse loading. Similar conceptual studies have been carried out by several researchers, e.g. [9]-[13], to study the dynamic structural response of concrete structures. Here, though, the impact loading was also combined with static loading, investigating the residual response of the damaged beams. Similar studies have been done by, e.g. [14]-[15], but there the focus has not been on the residual static response and the number of static follow-up tests have been somewhat limited. Another addition is the use of Digital image correlation (DIC), used in both impact and static tests, to register the response of the loaded beams.

DROP WEIGHT IMPACT TESTS

EXPERIMENTAL SETUP

Drop weight impact tests were conducted on 2 x 6 beams according to Fig. 1. The beam length was 1 180 mm with a span length of 1 000 mm, and a cross-sectional area of 100 x 100 mm^2. All beams were reinforced with four longitudinal ribbed bars with a nominal diameter of 6 mm and steel class K500C-T, located with 20 mm from the centre of the bars to the concrete surface. The beams were supported on cylindrical rollers, free to roll against the underlying rigid surface, with a diameter of 70 mm. The drop weight consisted of a non-solid steel cylinder with mass 10.1 kg (length: 260 mm, diameter 80 mm, radius at contact surface 400 mm). For further details of the experiments, see [17].

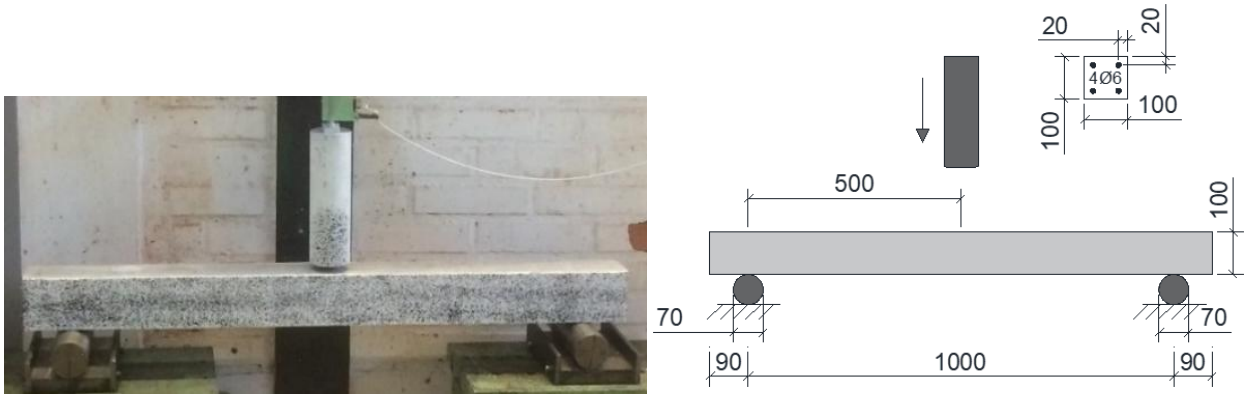

Fig. 1. Experimental setup for drop weight tests.

TEST SERIES

The reinforced concrete beams were casted in two batches with denotations in accordance with Table 1. Series-1 and Series-2 were first subjected to drop weight impact tests from two different heights, and thereafter statically tested in three-point bending until failure. In Series-1 and Series-2 a drop height of h = 2.5 m and h = 5.0 m, respectively, were used. After these impact tests the beams were subjected to static three-point bending until failure, and the results were compared with that of reference beams in Series-3, subjected to statically loading only using the same test set-up.

Table 1. Test series for drop weight impact tests and static tests.

Specimen	Batch	Series	Type of test	Drop height, h [m] [1)]
B-01, B-02, B-03	1	1	Impact	2.5
B-04, B-05, B-06	1	2	Impact	5.0
B-07, B-08, B-09	1	3	Static	-
B-10, B-11, B-12	2	1	Impact	2.5
B-13, B-14, B-15	2	2	Impact	5.0
B-16, B-17, B-18	2	3	Static	-

[1)] Impact velocity: 7.0 m/s (h = 2.5 m); 9.9 m/s (h = 5.0 m).

HIGH SPEED IMAGING AND DIC

The structural response of the beams where analysed by Digital image correlation (DIC), both in the dynamic and the static tests. This measurement technique is typically used to measure displacement fields and surface strain fields both in planar two-dimensional situations using a single camera set-up (2D-DIC) and in three-dimensional situations using a stereoscopic camera set-up (3D-DIC). The basic idea behind DIC is to measure the deformation of a specimen under testing by analysing the deformation of a surface speckle pattern in a series of digital images acquired during loading. This is accomplished by tracking the position of discrete pixel subsets of the speckle pattern within the images. The unique grey value speckle pattern of each subset is used to perform correlation calculations in such a way that each subset can be tracked with sub-pixel accuracy from one image to the next for all stages. The deformations of the specimens are then calculated by correlating the positions and displacements of subsets in the undeformed reference image and the deformed images to produce a deformation vector field. A comprehensive description of the measurement technique can be found in e.g. [16].

The impact tests of the beams were investigated using 2D-DIC technique with a Photron FASTCAM SA4 high-speed camera. The camera was provided with a Tamron AF 28-75/2.8 lens, with the focal length set at 28 mm and the aperture at f/2.8 during the test. The camera was placed at a perpendicular distance of approximately 1780 mm from the surface of the tested beam. A camera resolution of 1024x304 pixels and an image acquisition rate of 5 000

frames per second (fps) were used, corresponding to a time resolution of 0.2 ms. The camera configuration corresponded to a field of view of approximately 1200x360 mm^2; i.e. slightly more than the entire beam length.
The images from the high-speed camera were analysed by DIC technique using the software GOM Correlate, [18]. The dimensions of each subset were 15x15 pixels and the subset step was five pixels, which corresponds to a subset size and data point spacing of approximately 18 mm and 6 mm, respectively. The displacement resolution was approximately 0.01 mm for both *x*- and *y*-displacement components, determined as the standard deviation between two static images of the specimen before loading.

In the static loading tests, 3D-DIC measurements with a stereoscopic camera set-up were performed with the system ARAMIS 12M by Gom, [18]. The cameras had a resolution of 4096x3072 pixels and were proved with Titanar lenses with a focal length of 24 mm. The system configuration was calibrated for a field of view of approximately 1050x820 mm^2, covering slightly more than the distance between the supports. The images were captured with a frequency of 0.5 fps. The dimensions of each subset were 15x15 pixels and the subset step was 10 pixels. For the system configuration employed, this corresponds to a subset size and a data point spacing of approximately 3.7 mm and 2.5 mm, respectively, at the surface of the beam. The displacement resolution was determined to approximately 0.003 mm for both *x*- and *y*-displacement components and approximately 0.006 mm for *z*-displacement.

The speckle pattern used for the subset correlations was achieved by first applying white retro reflective paint as background and then, black stains using a natural sponge. Due to the higher resolution for the camera used in the static tests, a finer pattern was used for the specimens in Series-3. To obtain high contrast levels, the specimen was illuminated by a high-power white LED light panel while testing.

Material properties

Material properties for the concrete and the reinforcement are given in Table 2. The aim was to use concrete of class C30/37, [19], and reinforcement of steel class K500C-T was used for the beams. The values given in the table correspond to an average value of several material tests and the time of the drop weight impact tests were 36 days after casting the beams. Further details of the material tests are given in [17].

Table 2. Material properties for concrete and reinforcement steel.

Property	Description	Value
$f_{cm,cube,28}$	Mean compressive cube strength, 28 days	50.6 MPa
$f_{cm,cube,36}$	Mean compressive cube strength, 36 days	52.7 MPa
$f_{ctm,sp,36}$	Mean splitting tensile strength, 36 days	4.1 MPa
$G_{f,36}$	Fracture energy, 36 days	132 Nm/m^2
f_t	Ultimate tensile strength	686 MPa
$f_{0.2}$	Proof stress	575 MPa
E_{sm}	Modulus of elasticity	196 GPa
ε_{su}	Strain at ultimate tensile strength	10.8%

RESULTS

OVERVIEW

From images taken with the high-speed camera, DIC were used to measure the deformations of the beams and to show crack patterns obtained due to impact loading. The largest cracks were acceptably captured but for minor cracks, e.g. cracks in the top of the beam at initial loading, the resolution used turned out to be somewhat too low and such cracks could not be clearly observed.

DEFORMATION-TIME RELATIONS FROM IMPACT LOADING

The midpoint deformation over time for the impact loaded beams are shown in Fig. 2. The scatter of the results was small until maximum deformation was reached and the scatter increased somewhat after that. Failure was not reached, and the average maximum deformation (plastic deformation) was about 10.7 mm (4.7 mm), and 20.1 mm (12.5 mm) for Series-1 and Series-2, respectively.

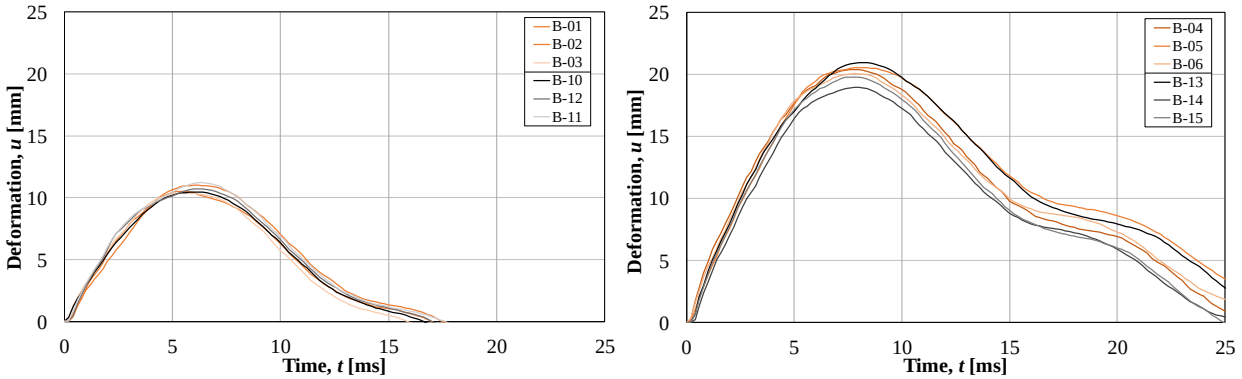

Fig. 2. Midpoint deflection over time for (a) Series-1, drop height h = 2.5 m, and for (b) Series-2, drop height h = 5.0 m.

INITIAL RESPONSE AT IMPACT LOADING

The initial response of a beam subjected to impact loading may differ much from that obtained in a beam subjected to static loading. This is also clearly seen in Fig. 3, in which the relative deformation of beam B-06 (Series-2) is shown for the initial 2.0 ms after impact. The deformation has here been normalized in relation to the corresponding maximum deformation for each time step and adjusted to zero deformation at the left support.

From this it is evident that the impact loaded beam does not obtain the typical triangular deformation shape expected for a beam that exhibit a plastic hinge in the middle of the beam. Initially, the beam parts close to the supports have hardly reacted to the applied impact load, resulting in mainly the middle part of the beam deforming. This generates a local negative curvature on both sides of the impact zone, approximately half way to the supports, and with time the region with negative curvature moves towards the supports. This phenomenon can be looked upon as the effect of time dependent boundary conditions; i.e. the boundary conditions can approximately be regarded as fixed with the location of the fixity moving closer to the real supports with time. Eventually, the beam become fully “aware” of the real supports and the response then changes to something more like that of a statically loaded beam. For the beam in Fig. 3 this change is deemed to be completed after about 2 ms.

The local negative curvature in the beam results in tensile stresses which may cause cracking in the top of the beam. Such cracks are also indicated in Fig. 4, showing the maximum principal strain fields from a DIC analysis.

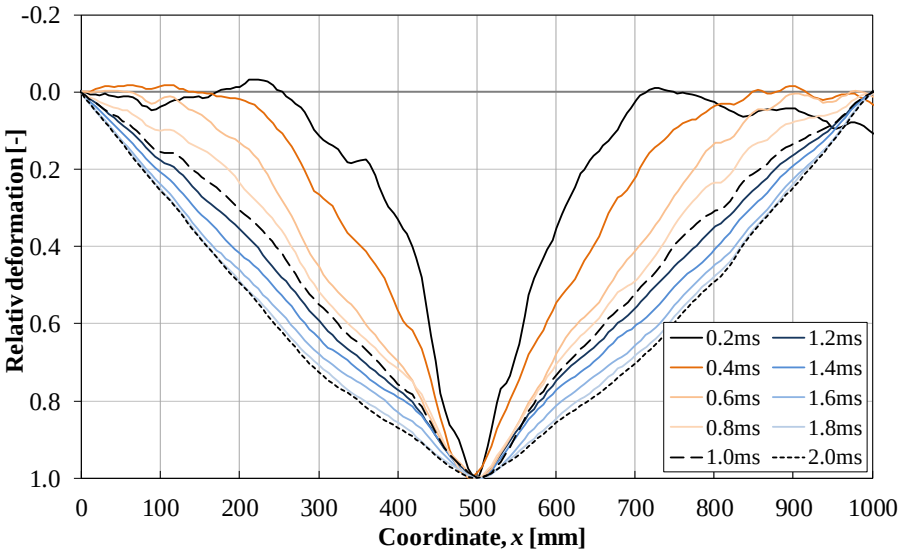

Fig. 3. Relative deformation of beam B-06 at different times after impact. Series-2, drop height of h = 5.0 m.

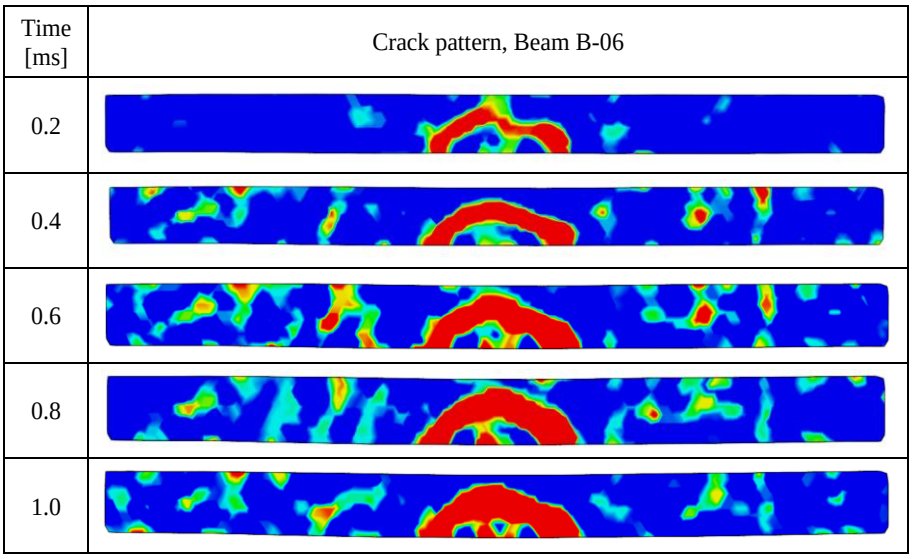

Fig. 4. Initial crack pattern of beam B-06 when subjected to impact loading. Cracks on the upper side of the beam is indicated.

LOAD-DEFORMATION RELATIONS FROM STATIC LOADING

The beams that were subjected to an impact load were afterwards statically loaded to evaluate their residual load-deformation properties; especially the residual strength and remaining plastic deformation capacity. The results are compared with the corresponding reference beams, Series-3, that were subjected to static loading only. In Fig.5 the resulting load-deformation relations are plotted for the beams in Series-1. The beams were cast in two different batches and the results are shown separately for each batch. Results from Series-3, using the average values and min/max envelopes from all six beams, are also shown as comparison. For the beams previously subjected to impact loading, a plastic deformation already existed, indicated in the graphs as an initial deformation at zero static load.

The initial elastic stiffness of the beams in Series-1 was very similar to that obtained in the cracked, static reference beams. When reaching a load level corresponding to that of the load-deformation relation of Series-3 the response became nonlinear and showed similar behaviour until failure. The ultimate load capacity and the plastic deformation capacity were in the same order as for the reference beams.

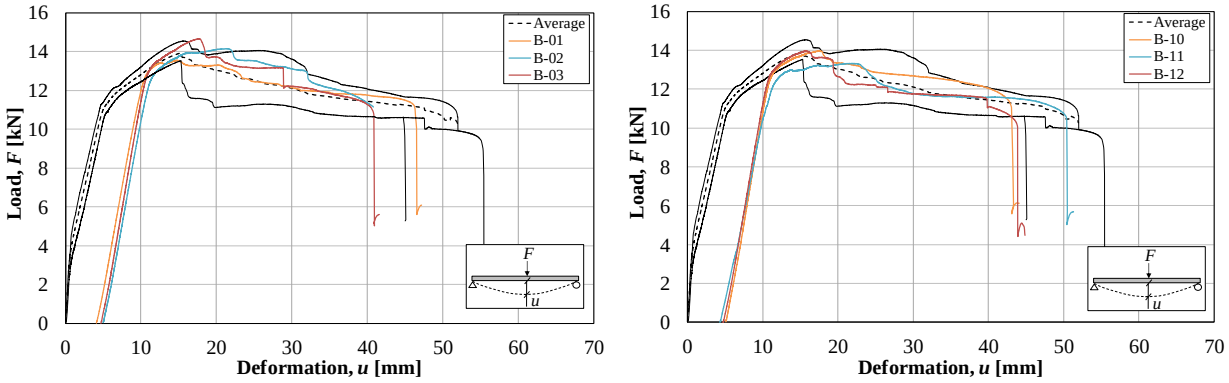

(a) (b)

Fig. 5. Comparison of load-deflection curves of (a) Series-1, batch 1 and (b) Series-1, batch 2, with Series-3, static references. Series-1, drop height of h = 2.5 m.

The resulting load-deformation relations for Series-2 are shown in Fig. 6 together with results from the static reference beams. These beams were also cast from two different batches and thus the results are shown separately for each batch.

The linear elastic stiffness decreased somewhat compared to that of the cracked reference beams. Once reaching a load level corresponding to the load-deformation relation of Series-3 the response became nonlinear and a response similar to that of the reference beams were obtained. For Series-2, though, the ultimate load capacity was somewhat reduced due to damage obtained by the beams in the previous impact loading. However, contrary to the beams with the lower drop height, the plastic deformation capacity increased compared to what were obtained in the static references. Final failure was in four cases reached due to torn off reinforcement.

The theoretical shear capacity was higher than the bending capacity, and thus bending failure was expected for all beams. Of all the beams tested, 17 out of 18 failed in bending (16 due to ruptured reinforcement; one was aborted prior to failure due to large deformations). However, in one beam (B-13) first subjected to impact loading, a shear failure unexpectedly occurred. Using DIC it was found that the previous impact loading had caused a diagonal shear crack to develop in a section located near the beam's quarter point. When subjected to static loading, this shear crack opened and eventually caused the beam to fail in shear at a much lower load level than that of the other beams.

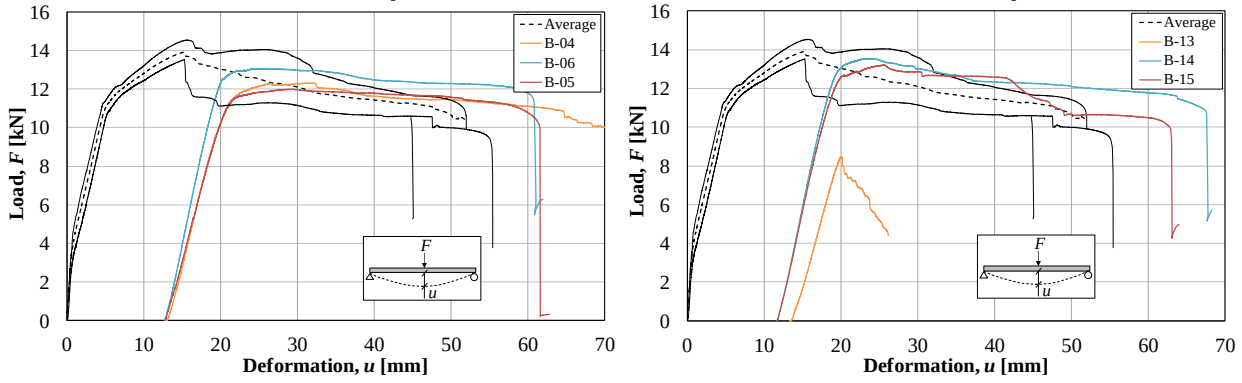

(a) (b)

Fig. 6. Comparison of load-deflection curves of (a) Series-2, batch 1 and (b) Series-2, batch 2, with Series-3, static references. Series-2, drop height of h = 5.0 m.

CRACK PATTERNS FOR STATIC LOADING

Crack patterns can be shown in GOM Correlate by showing the maximum principal strain field. Crack patterns for the static reference beams (Series-3) are shown in Fig. 7, and for the beams that were first subjected to impact loading, the crack patterns after static loading are shown in Fig. 8 (Series-1) and Fig. 9 (Series-2). Red and blue colour indicates a true crack and uncracked concrete, respectively. The crack patterns are shown at a load level $F_{95\%}$, equivalent to 95 % of the peak load, on the descending branch of the load-deformation relation. For orientation, the corresponding deformation, $u_{95\%}$, is given as well for each beam.

For the static loaded reference beams in Fig. 7, typical vertical flexural cracks and inclined flexural shear cracks can be observed.

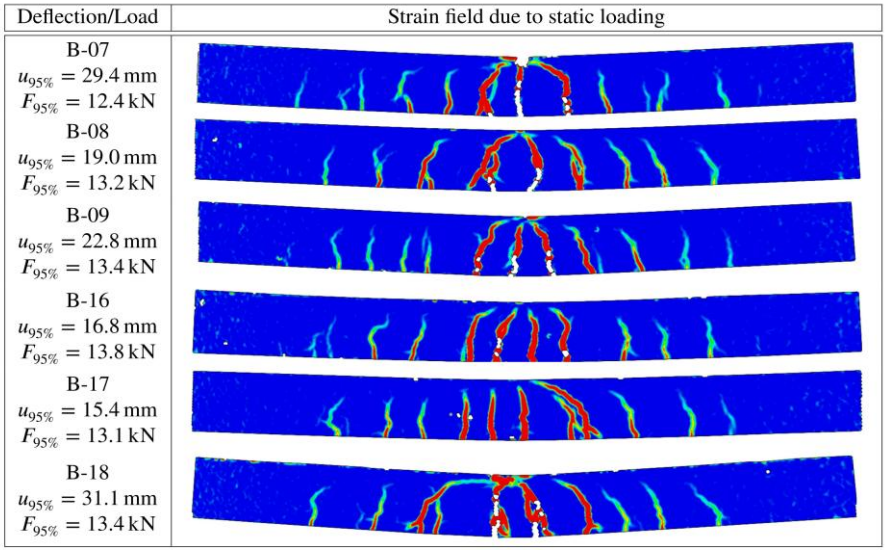

Fig. 7. Crack patterns for Series-3 (reference beams), static loading.

For the beams in Fig. 8 and Fig. 9 the initial crack patterns obtained were created during impact loading. During the following static loading the existing cracks re-opened and continued to grow.

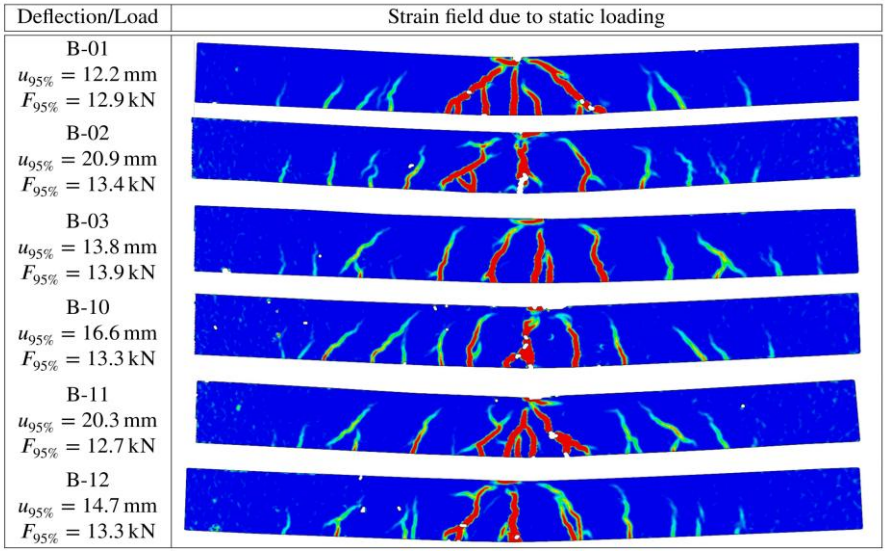

Fig. 8. Crack patterns for static loading after subjected to impact loading, Series-1, drop height h = 2.5 m.

For the beams subjected to lower impact load (Serie-1), see Fig. 8, the crack patterns obtained are not fully consistent. Some of the beams exhibited inclined shear cracks close to the impact zone, while some of the specimen, e.g. B-03 and B-10, obtained crack patterns very similar to that of the static reference beams. It can also be noted that the beams that experienced clearest inclined cracking, B-01 and B-11, were the same beams that also obtained the largest plastic deformation capacity prior to failure, see Fig. 5.

For the beams subjected to higher impact load (Series-2) the inclined cracks became more prominent as shown in Fig. 9. For these beams the number of cracks formed was less than that obtained in the other tests. Nevertheless, the plastic deformation capacity still increased compared to that of the reference beams, see Fig. 6. This is believed to be at least partly due to the presence of inclined cracks.

For two of the beams, B-13 and B-15, dominant shear cracks developed in a section located near the beam's quarter point. For beam B-13, this shear crack developed further during static loading and caused a premature shear failure, reducing the beam's load capacity considerably, see Fig. 6.

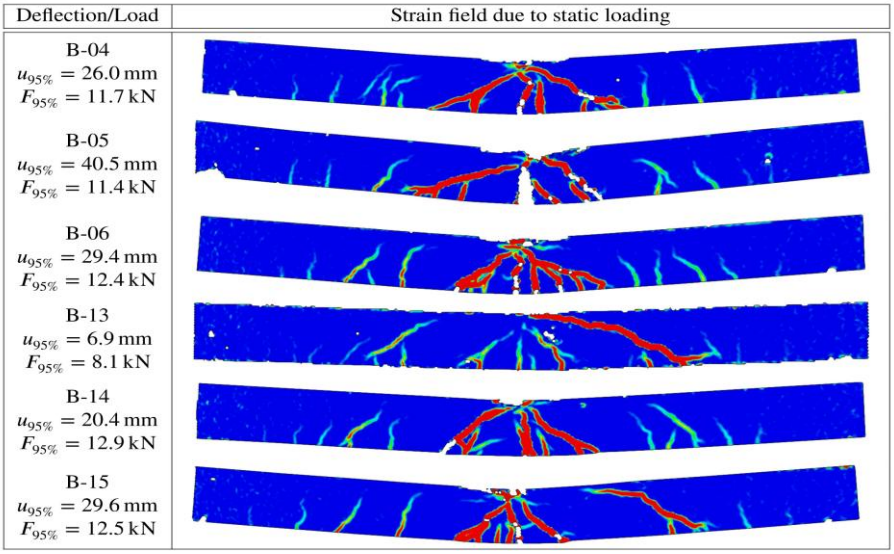

Fig. 9. Crack patterns for static loading after subjected to impact loading, Series-2, drop height h = 5.0 m.

CONCLUSIONS

High-speed camera in combination with Digital Image Correlation (DIC) analysis is a powerful tool for studying the structural response of impact loaded concrete beams. DIC can be used to study e.g. crack propagation, deformations, velocities or accelerations. It is important that the resolution is high enough if the aim is to capture the crack propagation; to study deformations, though, a lower resolution can be accepted. An additional advantage with DIC is that the parameters that are of interest do not need to be known or specified beforehand; i.e. if images of acceptable resolution are available it is possible to determine what type of results are of interest at a later stage. Consequently, compared to conventional measuring techniques, this is a considerable advantage.

The main aim was to study the residual plastic deformation capacity of beams first subjected to impact loading; and this was done with high accuracy using DIC analysis. For the impact load tests, a high-speed camera with capacity of 5 000 fps was used to register the results, and for static loading, two cameras were used with 0.5 fps. In the latter both deformations and crack propagation was captured very well. The resolution used in the high-speed camera, though, turned out to be somewhat too low to adequately study the full crack formation caused by the impact load. This was a negative side effect of the decision to capture the response of the whole beam during impact loading. The deformations were obtained well, and the largest cracks were acceptably captured, but the smaller cracks were not clearly observed using DIC.

Two different drop heights were used for the impact tests. After the beams were subjected to impact loading the beams were tested statically in three-point bending. The beams subjected to lower impact load showed similar response as the reference beams that were subjected to static loading only; the initial elastic stiffness and the ultimate load capacity were both similar to each other. For the beams subjected to higher impact load, though, the elastic stiffness and the ultimate load capacity were somewhat reduced. The results support the idea that the structural response of a structure previously subjected to an impact load, i.e. being partly damaged, will be similar to that obtained in a structure subjected to static loading only.

Furthermore, the residual plastic deformation capacity during the static tests was in the same order for the beams that were subjected to a lower impact load as the reference beams that were subjected to static loading only. For the beams subjected to a higher impact load, the residual plastic deformation capacity was higher compared to the static reference beams. It is believed that the increased plastic deformation capacity is due to positive effects related to diagonal shear cracks close to the impact zone. Consequently, a larger part of the reinforcement may reach yielding and, thus the length of the plastic hinge increases; resulting in larger plastic deformation capacity. This thought is further supported by the fact that beams with lower impact load, which exhibited inclined shear cracks got, somewhat higher plastic deformation capacity compared to beams obtaining just straight bending cracks.

The failure mode can be influenced by the type of loading. For one of the beams first subjected to higher impact load, shear failure occurred at a load level considerably lower than the expected load capacity obtained due to bending failure. This indicates that there might be a risk that preceding impact loading, even though theoretically not critical, may cause such damage that the residual strength of the affected structure is considerably reduced.

ACKNOWLEDGEMENTS

This research has been carried out in collaboration with Chalmers University of Technology and RISE Research Institutes of Sweden. The research is financed by the Swedish Civil Contingencies Agency. The authors would like to thank the financier, specially Lars Gråbergs, B.Sc. from Swedish Civil Contingencies Agency. Thanks also to Fortifikationskårens forskningsfond (Fortification corps' research fund) for additional financing of the experiments. Thanks, are also due to research engineer M.Sc. Sebastian Almfeldt at Chalmers, responsible for carrying out the experiments, and Ph.D. Ingemar Löfgren at Thomas Concrete Group, for providing the concrete mixtures and material for the beams. Additionally, Ph.D. Leo Laine, member of the West Coast Sweden Shock Wave Group (WCSSWG) are highly acknowledged for his input.

REFERENCES

[1] P. H. Bischoff and S.H. Perry (1991): "Compressive behaviour of concrete at high strain rates", *Materials and Structures*, 24, pp. 425-450.

[2] L. J. Malvar and C. A. Ross (1998): "Review of strain rate effects for concrete in tension", *ACI Materials Journal*, Vol. 95, No. 6, pp. 735-739.

[3] D. M. Cotsovos, N.D. Stathopoulos and C. A. Zeris (2008): "Behavior of RC Beams Subjected to High Rates of Concentrated Loading", *J Struct Eng*; 134: 1839–1851.

[4] P. Isaac, A. Darby, T. Ibell and M. Evernden (2017): "Experimental investigation into the force propagation velocity due to hard impacts on reinforced concrete members", *Int J Impact Eng*; 100: 131–138.

[5] T. M. Pham and H. Hao (2017): "Plastic hinges and inertia forces in RC beams under impact loads", *Int J Impact Eng*; 103: 1-11.

[6] DOD: *Structures to Resist the Effects of Accidental Explosions, UFC 3-340-02*. Department of Defense, USA.

[7] Fortifikationsverket (2011), *Fortifikationsverkets konstruktionsregler FKR 2011* (Swedish Fortifications Agency Building Regulations FKR 2011. In Swedish). Dnr 4535/2011, Eskilstuna, Sweden.

[8] M. Johansson (2015): *Impulsbelastade konstruktioner – Moment och tvärkraft* (Impulse loaded structures – Moment and shear force. In Swedish). Swedish Civil Contingencies Agency, Document B06-201, 2015-08-06, Karlstad, Sweden.

[9] L. Ågårdh, K. G. Bolling and L. Laine (1997): *Fibre reinforced concrete beams loaded by impact, 343 Experiments and FE-modelling*. Defence research establishment, FOA-R--9700587-344 311--SE, Tumba, Sweden.

[10] A. Ansell A and G. Svedbjörk (2001): *Dynamisk provning av fritt upplagda plattstrimlor av betong med armering av varierande seghet*. (Dynamic testing of simply supported concrete slab strips with reinforcement

of various ductility. In Swedish), Department of Concrete Structures, Royal Institute of Technology, Stockholm, Sweden.

[11] S. Saatci and F. Vecchio (2009): "Effects of shear mechanisms on impact behavior of reinforced concrete beams", *ACI Struct J*; 106: 78–86.

[12] K. Fujikake, B. Li and S. Soeun (2009): "Impact Response of Reinforced Concrete Beam and Its Analytical Evaluation", *J Struct Eng*;135: 938–950.

[13] G. S. D. Ulzurrun and C. Zanuy (2017): "Enhancement of impact performance of reinforced concrete beams without stirrups by adding steel fibers", *Constr Build Mater*; 145: 166–182.

[14] K. Fujikake, T. Senga, N. Ueda, T. Ohno and M. Katagiri (2006):" Study on Impact Response of Reactive Powder Concrete Beam and Its Analytical Model", *J of Adv Concrete Tech*, Vol 4, no.1, 99-108.

[15] S. D. Adhikary, B. Li, K. Fujikake (2015): "Residual Resistance of impact damaged reinforced concrete beams", *Mag of Concrete Research*, Vol 67, no 7, 364-378.

[16] M. A. Sutton, J. J. Orteu and H. Schreir (2009): *Image Correlation for Shape, Motion and Deformation Measurements*. Springer US, New York.

[17] F. J. Lozano and J. A. Makdesi (2017): *Concrete Beams Subjected to Drop-Weight Impact and Static Load*. Master's Thesis BOMX02-17-21, Department of Architecture and Civil Engineering, Chalmers University of Technology, Gothenburg, Sweden.

[18] Software GOM Correlate. n.d. http://www.gom.com/3d-software/gom-correlate.html

[19] CEN (2005): *Eurocode 2: Design of Concrete Structures – Part 1-1: General rules and rules for buildings*. European Committee for Standardization, EN 1992-1-1:2005, Brussels, Belgium.